DOI: 10.1002/chem.200800993

Design of Protonated Polyazamacrocycles Based on Phenanthroline Motifs for Selective Uptake of Aromatic Carboxylate Anions and Herbicides

Carla Cruz,[a] Vânia Calisto,[a] Rita Delgado,[b, c] and Vítor Félix*[a]

Abstract: Three novel large polyazamacrocycles containing two 1,10-phenanthroline (phen) units connected by two polyamine spacers of different length, [32]$phen_2N_4$, [30]$phen_2N_6$ and Me_2[34]$phen_2N_6$, have been synthesised and their protonated forms used as receptors for binding studies with several aromatic carboxylate anions (benzoate (bzc^-), 1-naphthalate ($naphc^-$), 9-anthracenate ($anthc^-$), pyrene-1-carboxylate ($pyrc^-$), phthalate, (ph^{2-}), isophthalate (iph^{2-}), terephthalate (tph^{2-}), 2,5-dihydroxy-1,4-benzenediacetate ($dihyac^{2-}$) and, 1,3,5-benzenetricarboxylate (btc^{3-})) and three herbicides (4-amino-3,5,6-trichloropyridine-2-carboxylate ($ATCP^-$), dichlorophenoxyacetate (2,4-D^-) and glyphosate (PMG^{2-})) in water solution. The [30]$phen_2N_6$ receptor was found to be the most suitable for binding the anions considered in a 1:1 stoichiometry. The three receptors exhibit a remarkable binding selectivity towards the extended aromatic anion $pyrc^-$ at low pH values. Their binding affinities for the monocarboxylate anions decrease with the extension of the aromatic system in the order $pyrc^- > anthc^- > naphc^- > bzc^-$, which indicates the presence of π–π stacking interactions in the molecular recognition of these anions. Molecular dynamics simulations carried out for the binding of $\{H_4$[30]$phen_2N_6\}^{4+}$ and $\{H_6Me_2$[34]$phen_2N_6\}^{6+}$ with $pyrc^-$, $anthc^-$, $naphc^-$, iph^{2-} and btc^{3-} in water showed that these receptors adopt a folded conformation with the anion inserted between the two phen heads and that the molecular recognition is governed by π–π stacking interactions and multiple N–H···O=C hydrogen bonds. The binding free energies estimated theoretically are very similar to those found by potentiometric methods, which supports the proposed binding arrangement.

Keywords: anions · molecular dynamics · molecular recognition · pi interactions · receptors

Introduction

Anion recognition by cationic receptors is, nowadays, an active area of research.[1–3] Aromatic carboxylate anions are widespread environmental contaminants of agricultural land causing ground water contamination that disrupts aquatic life cycles.[3–6] For example, the herbicide 4-amino-3,5,6-trichloropyridine-2-carboxylic acid, H(ATCP), commonly used to control deeply rooted herbaceous weeds and woody plants, pastures, and small grain crops, is very toxic and is rapidly absorbed from ground water.[4]

Thus, the development of receptors capable of sensing and extracting pollutants containing carboxylate groups with environmental impact, such as herbicides and pesticides, is essential.[7–9] However, these types of anions have a variety of special features, such as charge, size, pH dependence, solvation and geometry, that should be taken into account in the molecular design of receptors capable of their effective uptake.[10–12] With this main goal in mind, we have been involved in the development of artificial receptors containing phenanthroline (phen) units linked through polyaza alkyl spacers (Scheme 1). The protonated forms of these receptors offer an apparently rigid structure and several potential N–H binding sites suitable for the uptake of carboxylate anions with different net charges and geometric binding requirements (see Scheme 2). Therefore the binding selectivity is assisted by a combination of multiple and cooperative inter-

[a] C. Cruz, V. Calisto, Prof. V. Félix
Departamento Química
CICECO and Secção Autónoma de Ciências da Saúde
Universidade de Aveiro, 3810-193 Aveiro (Portugal)
Fax: (+351) 234-370084
E-mail: vitor.felix@.ua.pt

[b] Prof. R. Delgado
Instituto de Tecnologia Química e Biológica, UNL
Apartado 127, 2781-901 Oeiras (Portugal)
E-mail: delgado@itqb.unl.pt

[c] Prof. R. Delgado
Instituto Superior Técnico
Av. Rovisco Pais, 1049-001 Lisboa (Portugal)
Fax: (+351) 21-4411277

Supporting information for this article is available on the WWW under http://dx.doi.org/10.1002/chem.200800993.

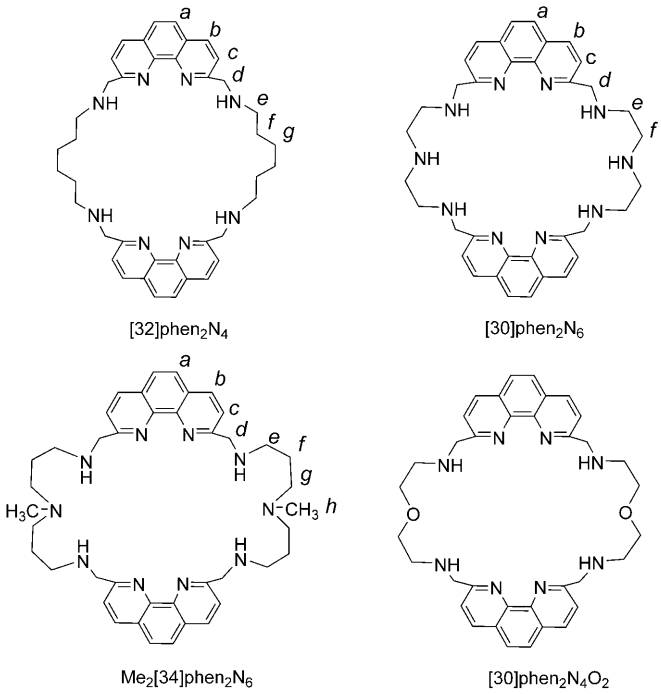

Scheme 1. Bis-phenanthroline macrocyclic receptors.

molecular interactions, such as hydrogen bonds and electrostatic and π–π stacking interactions.[13–15]

In a previous study we found that in the solid state the related dioxatetraaza $\{H_5[30]phen_2N_4O_2\}^{5+}$ receptor (see Scheme 1) accommodates chloride and bromide anions in a "horseshoe" shape conformation with the two phen rings adopting an almost parallel arrangement.[16] Furthermore, the results of solution binding studies with some aliphatic and aromatic anionic substrates suggested that this conformation is adopted in the binding of aromatic anions with extended π systems ($pyrc^-$) or high negative charge (btc^{3-}) leading to the formation of supermolecules with high association constants. By contrast, the affinity of this receptor for aliphatic anions is much lower, which suggests that other types of interactions and/or other conformational binding arrangements are adopted.[16] To obtain further insights into the dynamic binding behaviour, we present herein a comprehensive binding study of new receptors of this series, protonated $[32]phen_2N_4$, $[30]phen_2N_6$ and $Me_2[34]phen_2N_6$, with several aromatic anions (see Scheme 2), including the common herbicides $ATCP^-$ and $2,4\text{-}D^-$. For comparison purposes, an aliphatic herbicide PMG^{2-} was also considered. The anion-binding abilities of these receptors were evaluated by potentiometry and ^1H NMR spectroscopy and the association constants determined. The binding arrangements between the $\{H_4[30]phen_2N_6\}^{4+}$ and $\{H_6Me_2[34]phen_2N_6\}^{6+}$ receptors and selected anionic substrates ($pyrc^-$, $anthc^-$, $naphc^-$, iph^{2-} and btc^{3-}) in water solution were established by molecular dynamics simulations (MD). The entropic and enthalpic contributions to the binding free energies were estimated and compared with experimental values.

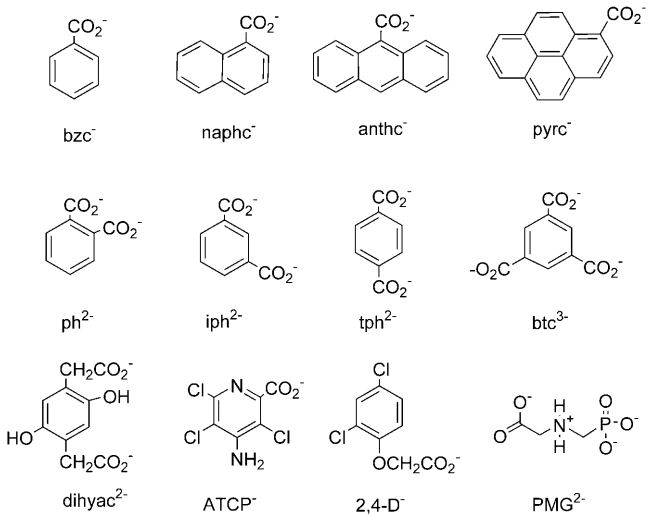

Scheme 2. Carboxylate and herbicide anions studied in this work.

Results and Discussion

Synthesis of receptors: The macrocycles $[32]phen_2N_4$, $[30]phen_2N_6$ and $Me_2[34]phen_2N_6$ were prepared by [2+2] cycloaddition reactions of 1,10-phenanthroline-2,9-dicarbaldehyde[17] with 1,6-hexanediamine, diethylenetriamine and *N,N*-bis(3-aminopropyl)methylamine, respectively, followed by reduction with sodium borohydride, as described for related compounds.[18] The macrocycles were isolated as chloride salts in yields of 80, 60 and 50%, respectively.

A few other related bis-phen macrocycles have been prepared from the same phen-dialdehyde derivative and different diamines[18] or by the reaction of 2,9-bis(chloromethyl)-1,10-phenanthroline and sulfonamide.[19] In the first case only Schiff bases were prepared, whereas in the second case, the small macrocycle obtained contains only two tertiary amines.

Acid–base properties of the receptors: The acid–base behaviour of the three macrocycles was studied by potentiometric methods in water for $[30]phen_2N_6$ and $Me_2[34]phen_2N_6$ and in H_2O/MeOH (50:50, v/v) for $[32]phen_2N_4$ at 298.2 K and an ionic strength of 0.10 M in KCl. The protonation constants were determined by using the HYPERQUAD program.[20] The overall protonation constants ($\log\beta_{H_hA_a}$) are given in Table S1 in the Supporting Information and the stepwise constants are listed in Table 1. Seven protonation constants were determined for $[30]phen_2N_6$ and $Me_2[34]phen_2N_6$ whereas only five were found for $[32]phen_2N_4$ in the 2–11 pH range.

The first four protonation constants for the three compounds are relatively high, with values ranging from 9.81 to 6.03. These values correspond to the successive protonation of the four secondary nitrogen atoms of the aliphatic amine linkages contiguous with the phen heads. The following two constants for the $[30]phen_2N_6$ and $Me_2[34]phen_2N_6$ macrocycles were assigned to the protonation of the remaining two

Table 1. Protonation constants ($\log K_i^H$)[a] for [32]$phen_2N_4$, [30]$phen_2N_6$ and Me_2[34]$phen_2N_6$ at $T=298.2$ K and $I=0.10$ M in KCl.

Equilibrium quotient	[32]$phen_2N_4$[b]	[30]$phen_2N_6$[c]		Me_2[34]$phen_2N_6$[c]
[HL]/[L][H]	9.76(1)	9.70(1)	9.36(3)[d]	9.81(1)
[H_2L]/[HL][H]	8.91(1)	8.86(1)	8.88(4)[d]	9.26(1)
[H_3L]/[H_2L][H]	7.86(1)	8.16(1)	8.06(6)[d]	8.21(1)
[H_4L]/[H_3L][H]	7.08(1)	6.03(1)	5.75(7)[d]	6.99(2)
[H_5L]/[H_4L][H]	2.09(2)	3.27(1)	3.30(5)[d]	6.29(1)
[H_6L]/[H_5L][H]	–	2.56(2)	2.59(4)[d]	5.70(1)
[H_7L]/[H_6L][H]	–	1.95(2)	2.16(4)[d]	1.84(2)

[a] The values in parentheses are standard deviations on the last significant figure. [b] Determined in H_2O/MeOH (50:50 v/v). [c] Determined in aqueous solution. [d] Determined by ^{1}H NMR titration in D_2O (see references [21,22]).

aliphatic nitrogen centres located in the middle of the triamine linkages. These constants for [30]$phen_2N_6$ are much lower than those found for Me_2[34]$phen_2N_6$ due to the shorter length of the chains between the amine centres in [30]$phen_2N_6$ and the consequent stronger electrostatic repulsion between the ammonium ions formed. The last constants, the fifth for [32]$phen_2N_4$ and seventh for [30]$phen_2N_6$ and Me_2[34]$phen_2N_6$, have been assigned to the protonation of a nitrogen donor from a phen unit as observed for the related receptor [30]$phen_2N_4O_2$.[16]

The acid–base behaviour of the three macrocycles is illustrated by their speciation diagrams[23] shown in Figure S1 in the Supporting Information. It is possible to see from these diagrams that the tetraprotonated form, H_4L^{4+}, is the main species in solution at pH≈4 for [32]$phen_2N_4$ and [30]$phen_2N_6$ whereas, at the same pH, compound Me_2[34]$phen_2N_6$ is completely in its hexaprotonated form, H_6L^{6+}. They also highlight the different behaviour of the three compounds at a pH below 6, which derive mainly from the low $\log K_5$ and $\log K_6$ values of [30]$phen_2N_6$ and result in a narrow pH range (4.0 to 5.2) in which $\{H_4[30]phen_2N_6\}^{4+}$ predominates.

The protonation sequence of [30]$phen_2N_6$ was confirmed by the ^{1}H NMR titration shown in Figure S2. The protonation constants were also determined with the HypNMR program[21] and they are compared in Table 1 with those determined by potentiometric methods. All the proton resonances (see Scheme 1 for the numbering) were assigned on the basis of NOESY experiments. Cross-peaks were observed between the doublet H_c resonance and the singlet H_d and triplet H_e resonances, which allowed the doublet at a lower field to be assigned to the H_b protons. It is apparent from the titration experiment that the first four successive protonations occur at the secondary amine centres adjacent to the phen rings, as the H_d, H_a and H_b resonances shift downfield as well as, but to a lesser extent, the H_c and H_f resonances. The next three protonations take place almost simultaneously at the central aliphatic nitrogen centres and at one of the nitrogen atoms of a phen unit, as revealed by the H_f and H_e resonance shifts as well as by the downfield shift of the three aromatic resonances. In fact, the protonation constants for the last three protonations are of the same order and occur in the same pD region. The fact that the phen protons start to shift at pD≈3, when the protonations mainly occur at the central amines, is also an indication that the macrocycle adopts a folded conformation.

Similar protonation schemes were also found for the related macrocycles R_2[30]$phen_2N_6$ (with *N*-pendant arms on the middle nitrogen atoms, R=2-(aminoethyl)-2-naphthalen-1-ylmehyl)[24] and [30]$phen_2N_4O_2$.[16] The protonation sequence and the calculated constants are entirely consistent with the potentiometric data.

Binding studies of the receptors with anionic substrates

Potentiometric measurements: The binding constants of the protonated forms of the macrocycles $\{H_i[32]phen_2N_4\}^{i+}$ ($i=2$–5), $\{H_j[30]phen_2N_6\}^{j+}$ and $\{H_jMe_2[34]phen_2N_6\}^{j+}$ ($j=2$–7) as receptors and the anionic substrates represented in Scheme 2 were determined at 298.2 K and an ionic strength of 0.10 M in KCl by using the HYPERQUAD program.[20] For the first receptor H_2O/MeOH (50:50 v/v) was used as the solvent for reasons of solubility, whereas the other two were studied in water. The binding constants determined and the corresponding equilibria are collected in Table S3 in the Supporting Information. The values of the protonation constants reported in the literature for the studied anions exhibit large discrepancies,[25] so that they were determined under the experimental conditions reported in this work. The values for most of the anions in water were presented earlier[16] and the new ones are compiled in Table S2 in the Supporting Information.

The receptors are able to interact with the anionic substrates to form several species with different protonation states, all of them with a 1:1 receptor/substrate stoichiometry, which was confirmed by a Job plot[26] (see Figure S3 in the Supporting Information). This indicates that the receptors and the anions take part in several overlapping protonation equilibria. The stepwise equilibria that effectively occur, for all those that can be established for each case, are unambiguously indicated by the plot of the effective binding constants (K_{eff}) as a function of pH, as described previously.[16,27–29] K_{eff} is defined as the quotient between the total amount of supramolecular species formed and the total amounts of the free receptor and free substrate at a given pH: $K_{eff}=\Sigma[H_nLA]/\Sigma[H_aA]\Sigma[H_iL]$ (in our case, $n=3$–8, $a=0$–3 and $i=0$–7). The plots for the studied systems are shown in Figure 1 and the effective equilibria for each system and the corresponding stepwise thermodynamic constants are compiled in Table 2. In fact several equilibria can be conceived taking into account the different protonated species available for each receptor and each anion leading to the same associated species as obtained with the model of the overall constants presented in Table S3. Therefore, it is essential to ascertain a criterion to choose the stepwise equilibria that have chemical significance, which is given by the K_{eff}, as described in ref. [16].

These results show that $\{H_i[32]phen_2N_4\}^{i+}$ is the weakest receptor for the anionic substrates studied and

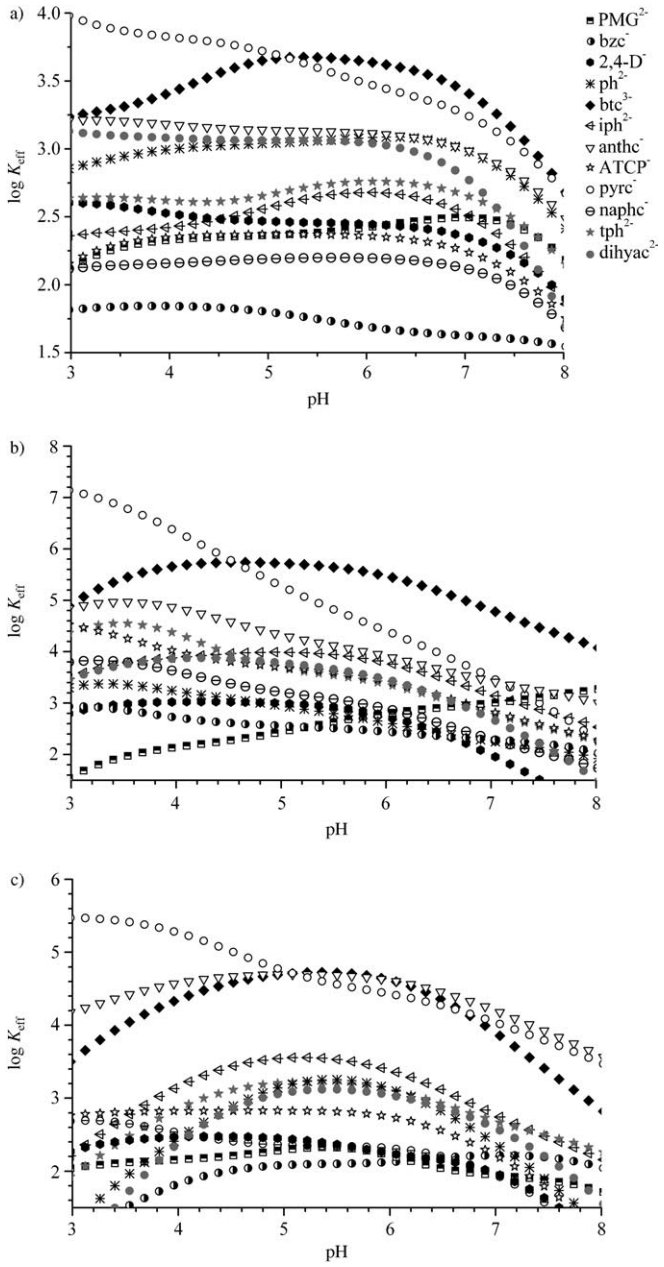

Figure 1. Plots of $\log K_{eff}$ values versus pH for the systems a) $\{H_i[32]phen_2N_4A\}^{i+}$, b) $\{H_i[30]phen_2N_6A\}^{i+}$ ($i=3$–7) and c) $\{H_jMe_2[34]phen_2N_6A\}^{j+}$ ($j=3$–8), with A the anionic substrates presented in Scheme 1 ($C_L=C_A=2\times10^{-3}$ M). The figure is presented in colour in the Supporting Information.

$\{H_j[30]phen_2N_6\}^{j+}$ is the best. This clearly shows the importance of the presence of the triammonium binding sites due to the higher electrostatic charge complemented by the suitable positions of the N–H groups for the establishment of N–H···O hydrogen bonds. The $\{H_j[30]phen_2N_6\}^{j+}$ receptor presents remarkably high binding affinities ($\log K_{eff}>7$ at pH 3 with pyrc$^-$ and 5.5 with btc^{3-} at pH≈4) and good selectivity between pyrc$^-$ and all the other anions studied, even btc^{3-} or anthc$^-$. This receptor also discriminates rather well the related substrates anthc$^-$ and naphc$^-$ (see below). Note that, in spite of the larger overall basicity of $\{H_jMe_2[34]phen_2N_6\}^{j+}$, which can be protonated at all of the six amine centres at pH≈4.5, this receptor does not exhibit the largest association constant with any of the studied anions. In contrast, $\{H_j[30]phen_2N_6\}^{j+}$, which at the same pH has only four ammonium centres, has the best affinity with almost all of the anions. This is a clear indication that electrostatic interactions, although important for the overall binding interaction of the anions, are not the most important contribution to the recognition of these partners. In addition, all three receptors exhibit larger affinities for three of the studied anionic substrates, pyrc$^-$, btc^{3-} and anthc$^-$. The $\{H_j[30]phen_2N_6\}^{j+}$ receptor also exhibits large affinities for tph^{2-} and ATCP$^-$ at pH<3.5 and for iph^{2-} and dihyac^{2-} at pH≈5.

The differences in binding interaction of the three receptors for the same anion are illustrated in Figure 2 for three anionic substrates, pyrc$^-$, btc^{3-} and ATCP$^-$, versus pH. The binding affinities for pyrc$^-$ with each of the three receptors are higher in the low pH range (up to 4), decreasing at higher pH values. In contrast, btc^{3-} becomes the preferred substrate for the $\{H_j[30]phen_2N_6\}^{j+}$ and $\{H_jMe_2[34]phen_2N_6\}^{j+}$ receptors at pH>4.5. On the other hand, the $\{H_jMe_2[34]phen_2N_6\}^{j+}$ receptor exhibits similar effective binding constants for btc^{3-}, pyrc$^-$ and anthc$^-$ at pH values between 4.5 and 6.5, but above pH 6.5 the affinity of this receptor for the two extended aromatic anions is definitely more favourable (see Figure 1). These results suggest π–π stacking interactions between the phen fragments of the receptors and the aromatic moiety of the anions are important interactions in the whole recognition process.

On the other hand, the $\{H_jMe_2[34]phen_2N_6\}^{j+}$ receptor presents not only lower binding constants with the studied anions when compared with $\{H_j[30]phen_2N_6\}^{j+}$, but also it poorly discriminates several pairs of anions (see Figure 1c), such as pyrc$^-$/btc^{3-}, btc^{3-}/ph^{2-}, pyrc$^-$/anthc$^-$ or anthc$^-$/naphc$^-$, which can be readily separated by $\{H_j[30]phen_2N_6\}^{j+}$ (at pH≈3, 5, 2 and 2, respectively). These conclusions concerning the selectivity of the receptors can be better visualised by competitive binding diagrams,[29] which are presented as selectivity plots of the overall percentages of the associated species as a function of pH for systems containing equimolecular amounts of one of the receptors and several anions.

The cases of $\{H_j[30]phen_2N_6\}^{j+}$ in solutions containing four anions, namely, a) btc^{3-}, pyrc$^-$, ATCP$^-$ and PMG^{2-} and b) pyrc$^-$, anthc$^-$, naphc$^-$ and bzc$^-$, are shown in Figure 3. The behaviour of the other two receptors in solutions containing the same mixtures of anions is shown in Figure S4 in the Supporting Information.

For these two mixtures of anionic substrates, $\{H_j[30]phen_2N_6\}^{j+}$ is the most appropriate for the selective uptake of btc^{3-} and pyrc$^-$ from the mixture (a) and for the selective uptake of pyrc$^-$ from the mixture (b). Indeed, the plot for this receptor for the mixture (a) displays an isoselectivity point at pH 4.5 at which the amounts of btc^{3-} and pyrc$^-$ bound to $\{H_j[30]phen_2N_6\}^{j+}$ are equal. The uptake of

Table 2. Stepwise binding constants ($\log K_{H_pL_rA_a}$) for the indicated equilibria.[a]

Reaction[b]	bzc^-	$naphc^-$	$anthc^-$	$pyrc^-$	ph^{2-}	iph^{2-}	tph^{2-}	btc^{3-}	$ATCP^-$	$2,4\text{-}D^-$	PMG^{2-}	$dihyac^{2-}$
						[32]$phen_2N_4$[c]						
$H_4L+H_3A\rightleftarrows H_7LA$	–	–	–	–	–	–	–	3.25(2	–	–	–	–
$H_4L+H_2A\rightleftarrows H_6LA$	–	–	–	–	2.81(2)	2.39(2)	2.67(2)	3.36(1)	–	–	2.36(3)	3.09(2)
$H_4L+HA\rightleftarrows H_5LA$	1.87(4)	2.15(6)	3.26(4)	3.82(3)	3.04(1)	2.46(2)	2.52(1)	3.75(1)	–	2.67(4)	–	3.05(2)
$H_4L+A\rightleftarrows H_4LA$	1.63(5)	2.21(4)	3.13(3)	3.42(2)	3.20(1)	2.74(1)	2.80(1)	3.65(1)	2.38(1)	2.46(4)	–	–
$H_3L+HA\rightleftarrows H_4LA$	–	–	–	–	–	–	–	–	–	–	2.59(3)	–
$H_3L+A\rightleftarrows H_3LA$	1.56(6)	2.06(5)	2.83(4)	2.99(3)	2.73(2)	2.14(3)	2.50(2)	2.91(2)	2.11(3)	2.27(6)	–	3.08(1)
						[30]$phen_2N_6$[d]						
$H_6L+HA\rightleftarrows H_7LA$	–	–	4.62(4)	–	–	–	–	–	–	–	–	–
$H_5L+H_2A\rightleftarrows H_7LA$	–	–	–	–	–	–	–	–	–	–	–	3.19(6)
$H_5L+HA\rightleftarrows H_6LA$	3.16(3)	3.88(2)	4.42(9)	7.27(5)	3.79(2)	–	5.02(5)	–	–	–	–	–
$H_4L+H_2A\rightleftarrows H_6LA$	–	–	–	–	–	–	–	5.45(1)	–	–	2.18(5)	3.90(3)
$H_4L+HA\rightleftarrows H_5LA$	2.79(4)	–	–	6.23(3)	3.09(2)	3.88(1)	3.81(4)	5.82(1)	–	–	2.81(4)	4.00(3)
$H_5L+A\rightleftarrows H_5LA$	–	–	–	6.96(3)	–	–	–	–	4.58(1)	3.13(2)	–	–
$H_4L+A\rightleftarrows H_4LA$	2.56(4)	3.15(3)	4.13(3)	4.52(4)	2.81(3)	4.06(1)	3.63(2)	5.75(1)	3.68(1)	3.04(1)	–	3.74(2)
$H_3L+H_2A\rightleftarrows H_5LA$	–	–	–	–	–	–	–	–	–	–	3.40(4)	–
$H_3L+HA\rightleftarrows H_4LA$	–	–	–	–	–	–	–	–	–	–	2.95(3)	–
$H_3L+A\rightleftarrows H_3LA$	2.29(4)	1.93(7)	3.24(3)	–	2.17(4)	2.71(2)	2.45(5)	4.21(1)	2.47(2)	–	–	–
						Me_2[34]$phen_2N_6$[d]						
$H_6L+H_2A\rightleftarrows H_8LA$	–	–	–	–	–	–	–	–	–	–	2.14(1)	–
$H_6L+HA\rightleftarrows H_7LA$	–	2.93(2)	3.96(1)	5.55(1)	–	2.55(2)	2.58(5)	4.27(1)	–	–	2.68(1)	–
$H_6L+A\rightleftarrows H_6LA$	2.14(3)	2.32(2)	4.73(1)	4.53(1)	3.51(1)	3.67(1)	3.31(1)	4.81(1)	2.83(1)	2.51(2)	–	3.26(1)
$H_5L+HA\rightleftarrows H_6LA$	–	–	–	–	–	–	–	–	–	–	2.07(1)	–
$H_5L+A\rightleftarrows H_5LA$	2.05(4)	2.39(1)	4.68(1)	4.47(1)	3.11(1)	3.38(1)	3.16(2)	4.72(1)	2.84(1)	2.03(5)	–	3.06(1)
$H_4L+HA\rightleftarrows H_5LA$	–	–	–	–	–	–	–	–	–	–	1.98(1)	–
$H_4L+A\rightleftarrows H_4LA$	–	2.20(2)	4.35(1)	4.18(1)	2.44(2)	2.82(2)	2.74(2)	3.83(2)	2.38(2)	2.28(3)	–	2.82(1)
$H_3L+A\rightleftarrows H_3LA$	–	–	3.64(1)	3.58(2)	–	2.28(2)	2.43(3)	2.66(4)	–	–	–	–

[a] L = [32]$phen_2N_4$, [30]$phen_2N_6$ and Me_2[34]$phen_2N_6$; A = anion. $I = 0.10$ M in KCl at 298.2 K. [b] Charges omitted for clarity. [c] Determined in H_2O/MeOH (50:50 v/v). [d] Determined in H_2O.

btc^{3-} is around 80% at pH values >4.5, whereas at pH 3.0 the uptake of $pyrc^-$ by this receptor is around 90% from the anionic mixture. On the other hand the uptake of $pyrc^-$ by $\{H_j[30]phen_2N_6\}^{j+}$ in the mixture (b) is almost 100% at pH 2. Through similar diagrams it is possible to see that $\{H_j[30]phen_2N_6\}^{j+}$ is the receptor that better discriminates between tph^{2-} and ph^{2-} (almost 80% at pH 3.5) or between $anthc^-$ and $naphc^-$ (about 80% at pH 2).

NMR measurements: The binding affinity process between $\{H_4[32]phen_2N_4\}^{4+}$, $\{H_4[30]phen_2N_6\}^{4+}$ and $\{H_6Me_2[34]phen_2N_6\}^{6+}$ with the bzc^-, $naphc^-$, ph^{2-}, iph^{2-}, tph^{2-}, btc^{3-}, $ATCP^-$, $2,4\text{-}D^-$ and PMG^{2-} anionic substrates was also evaluated by ^{1}H NMR titrations. Separated ^{1}H NMR signals were found for the receptor and the substrate protons upon formation of the receptor–substrate entity, which indicates a fast exchange between the free and associated species on the NMR timescale.

An illustrative example is shown in Figure 4 for the interaction of $\{H_4[30]phen_2N_6\}^{4+}$ with btc^{3-} at pD = 4.95. The formation of the supramolecular entity is accompanied by a significant broadening of the signals of the receptor and the anion. Moreover, the addition of the anion causes significant upfield shifts of the H_a, H_b and H_d resonances in relation to the free receptor, only minor changes in the H_c doublet and the two triplets from H_e and H_f move downfield. The ^{1}H NMR chemical shifts ($\Delta\delta = \delta_R - \delta_{obs}$) that result from the addition of solutions of the studied anions to the three receptors are listed in Table S4 in the Supporting Information. The pD was kept at 4 for $\{H_4[32]phen_2N_4\}^{4+}$ and ≈5 for the other two during the titrations, within ±0.25 pD units, at which the three receptors are in the protonated forms $\{H_4[32]phen_2N_4\}^{4+}$, $\{H_4[30]phen_2N_6\}^{4+}$ and $\{H_6Me_2[34]phen_2N_6\}^{6+}$, respectively, and most of the anions are deprotonated.

The titrations of the three receptors with the btc^{3-} and $ATCP^-$ substrates for the H_a and H_d resonances are shown in Figure 5. All the curve profiles are consistent with a 1:1 receptor/anion stoichiometry and this was confirmed by the Job plots.[26] The corresponding plots for $\{H_6Me_2[34]phen_2N_6\}^{6+}/btc^{3-}$ and $\{H_4[30]phen_2N_6\}^{4+}/ph^{2-}$ are included in Figure S3 in the Supporting Information.

The binding constants determined from the ^{1}H NMR titrations by using the HypNMR program[21] are compiled in Table 3. The values found are in good agreement with the corresponding constants obtained by potentiometric measurements, taking into account the fact that these titrations were performed in D_2O instead of water, the ionic strength was not controlled and no buffer was used to maintain the pH.

2D NMR experiments: The associations of bzc^-, $naphc^-$, ph^{2-}, iph^{2-}, tph^{2-}, btc^{3-}, $ATCP^-$, $2,4\text{-}D^-$ and PMG^{2-} with the $\{H_4[30]phen_2N_6\}^{4+}$ receptor were also studied by NOESY experiments. The supramolecular entities formed exhibit cross-peaks between the H_a, H_b, H_c and H_d resonances and all the resonances of tph^{2-} (singlet), bzc^- (two triplets and doublet) and iph^{2-} (singlet, doublet and triplet). With the re-

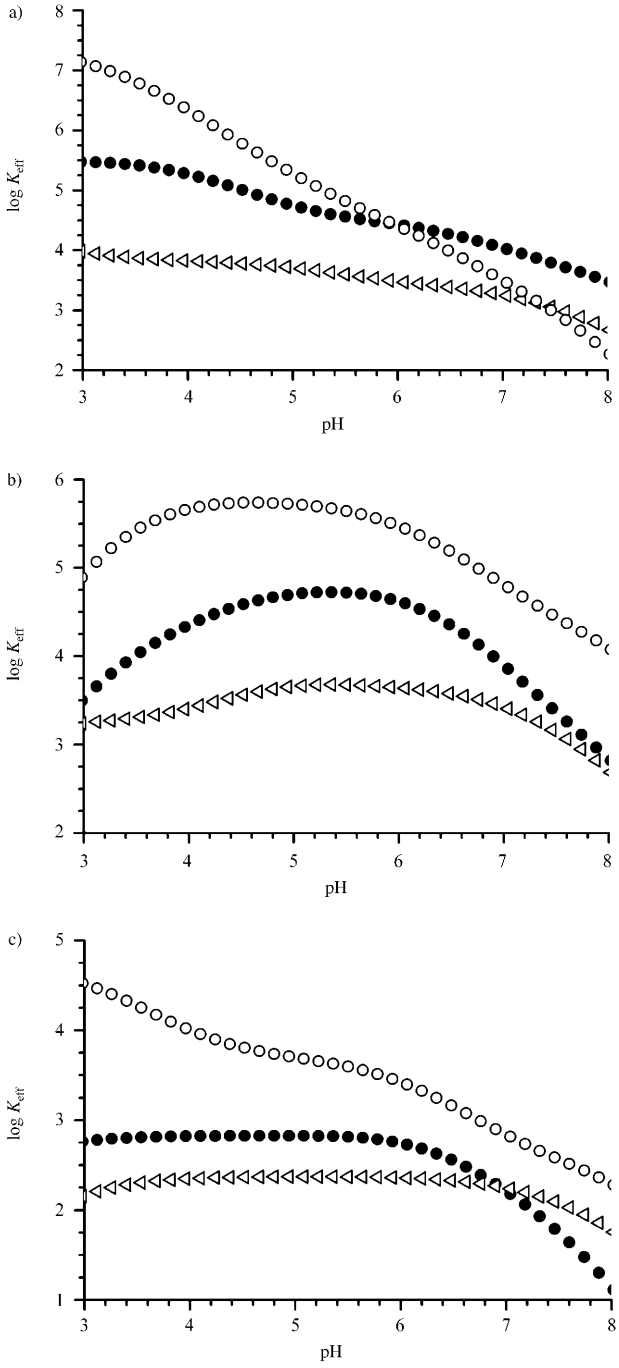

Figure 2. Plots of $\log K_{eff}$ versus pH for $\{H_i[32]phen_2N_4\}^{i+}$ (◁), $\{H_j[30]phen_2N_6\}^{j+}$ (●) and $\{H_jMe_2[34]phen_2N_6\}^{j+}$ (○) with a) $pyrc^-$, b) btc^{3-} and c) $ATCP^-$. The figure is presented in colour in the Supporting Information.

maining aromatic anions ($naphc^-$, btc^{3-}, ph^{2-} and 2,4-D^-) only strong cross-peak signals occur with the aromatic protons (H_a, H_b and H_c). These results suggest that these anions and the receptor are involved in π–π stacking interactions, which is consistent with a binding arrangement in which the anion is inserted between the two phen moieties, as shown below.

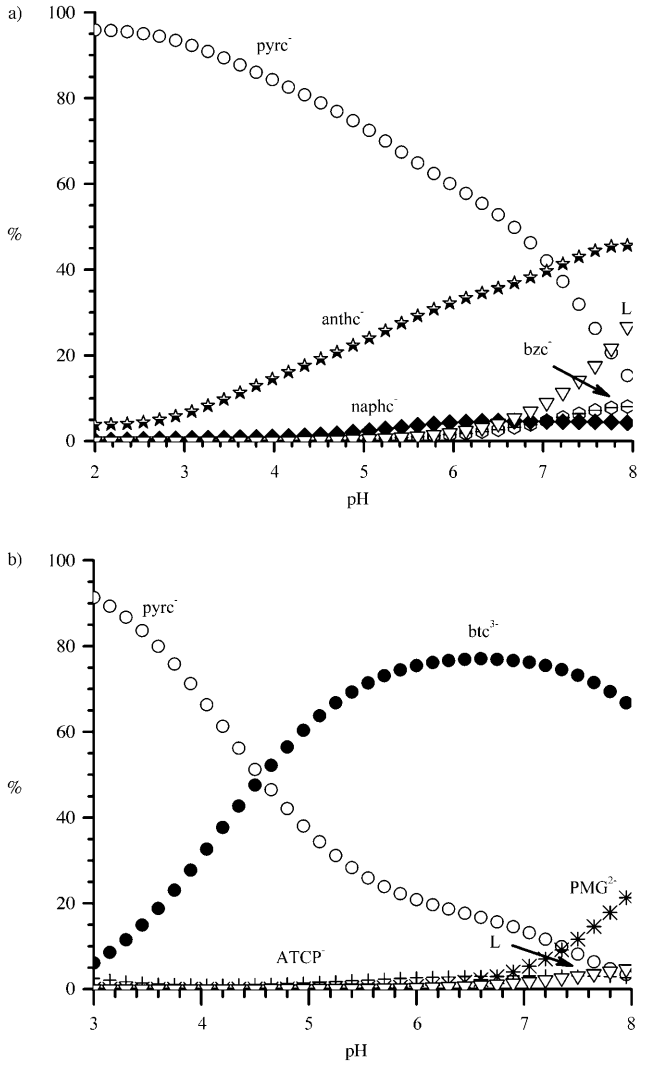

Figure 3. Overall percentages of the associated species of $\{H_j[30]phen_2N_6\}^{j+}$ as a function of pH in mixtures containing the following anions: a) $pyrc^-$, $anthc^-$, $naphc^-$ and bzc^- and b) btc^{3-}, $pyrc^-$, $ATCP^-$ and PMG^{2-}. The concentration of the receptor and each anion is 2×10^{-3} M. The figure is presented in colour in the Supporting Information.

In contrast, the interaction between $\{H_4[30]phen_2N_6\}^{4+}$ and the aliphatic herbicide PMG^{2-} is characterised by strong intermolecular NOE signals between the two singlets of the anion and the H_d, H_e and H_f resonances of the aliphatic part of the receptor, which suggests that PMG^{2-} interacts with the macrocycle through N–H···O hydrogen bonds. Some of the NOESY spectra are shown for this receptor in Figure S5 in the Supporting Information. Figures S6 and S7 also show the NOESY spectra of the associated entities formed by $\{H_4[32]phen_2N_4\}^{4+}$ with PMG^{2-} and $naphc^-$, and $\{H_6Me_2[34]phen_2N_6\}^{6+}$ with PMG^{2-} and 2,4-D^-.

X-ray single-crystal structure of $\{H_6[30]phen_2N_6\}^{6+}$ with the phthalate anion: The single-crystal X-ray diffraction structure of the supramolecular aggregate formed between $\{H_6[30]phen_2N_6\}^{6+}$ and the phthalate anion shows that its

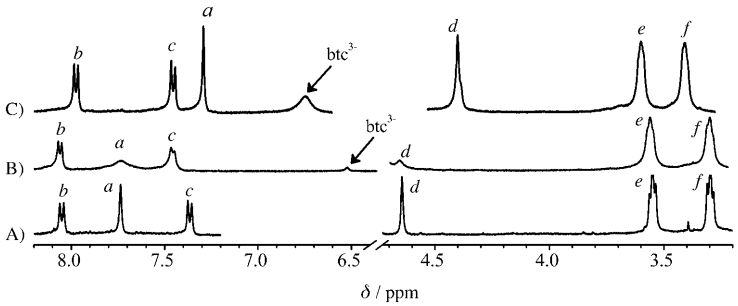

Figure 4. ^{1}H NMR spectra of A) the free receptor $\{H_4[30]phen_2N_6\}^{4+}$ in D_2O and B) upon the addition of 0.2 equiv and C) 1.0 equiv of btc^{3-} solution at pD = 4.95 ($C_R = 2.50\times10^{-3}$ M, $C_S = 2.65\times10^{-2}$ M).

Table 3. Binding constants ($\log K$)[a] for $\{H_4[32]phen_2N_4\}^{4+}$, $\{H_4[30]phen_2N_6\}^{4+}$ and $\{H_6Me_2[34]phen_2N_6\}^{6+}$ with the studied anions determined in D_2O at 300 K.

Anions	$\{H_4[32]phen_2N_4\}^{4+}$	$\{H_4[30]phen_2N_6\}^{4+}$	$\{H_6Me_2[34]phen_2N_6\}^{6+}$
bzc^-	1.92(2)	3.20(3)	1.97(2)
$naphc^-$	2.14(2)	3.54 (4)	2.60(1)
ph^{2-}	3.14(1)	3.33(4)	3.01(2)
iph^{2-}	2.51(2)	4.12(5)	3.40(3)
tph^{2-}	2.72(1)	3.83(3)	3.26(2)
btc^{3-}	3.84(5)	>5.0	4.55(5)
$ATCP^-$	2.47(1)	3.99(5)	2.85(1)
$2,4\text{-}D^-$	2.50(1)	3.08(5)	2.70(1)
PMG^{2-}	–	2.65(3)	2.16(3)

[a] Values in parentheses are standard deviations in the last significant figures given directly by the program.[21]

crystal structure is built from an asymmetric unit composed of one half of the macrocyclic cation, two aromatic anions and four water molecules. The receptor exhibits a crystallographic centre of symmetry with all six aliphatic N–H binding groups protonated. Furthermore, the charge balance requires an extra proton, crystallographically independent, located between the carboxylate groups of the two phthalate anions, which leads to the formation of the dimer [ph(μ-H)ph]$^{3-}$ with O···H distances of 1.20 and 1.26 Å and a O···O short distance of 2.45 Å. The O···H···O angle is 173°. The dimensions of these structural distances are similar to those found in the solid state of other dimers composed of benzoic acid derivatives.[30] Hence, the molecular formula of the supramolecular compound described is definitively $[\{H_6[30]phen_2N_6\}][ph(\mu\text{-}H)ph]_2\cdot 8H_2O$, with a receptor/anion ratio of 1:4, which is different to the equimolar stoichiometry found in the experimental binding studies and suggests that packing effects play an important role in the crystal structure. Nevertheless, suitable crystals for X-ray diffraction studies could only be grown from a solution containing an excess of phthalic acid. The overall structure of $[\{H_6[30]phen_2N_6\}][ph(\mu\text{-}H)ph]_2$ is shown in Figure 6.

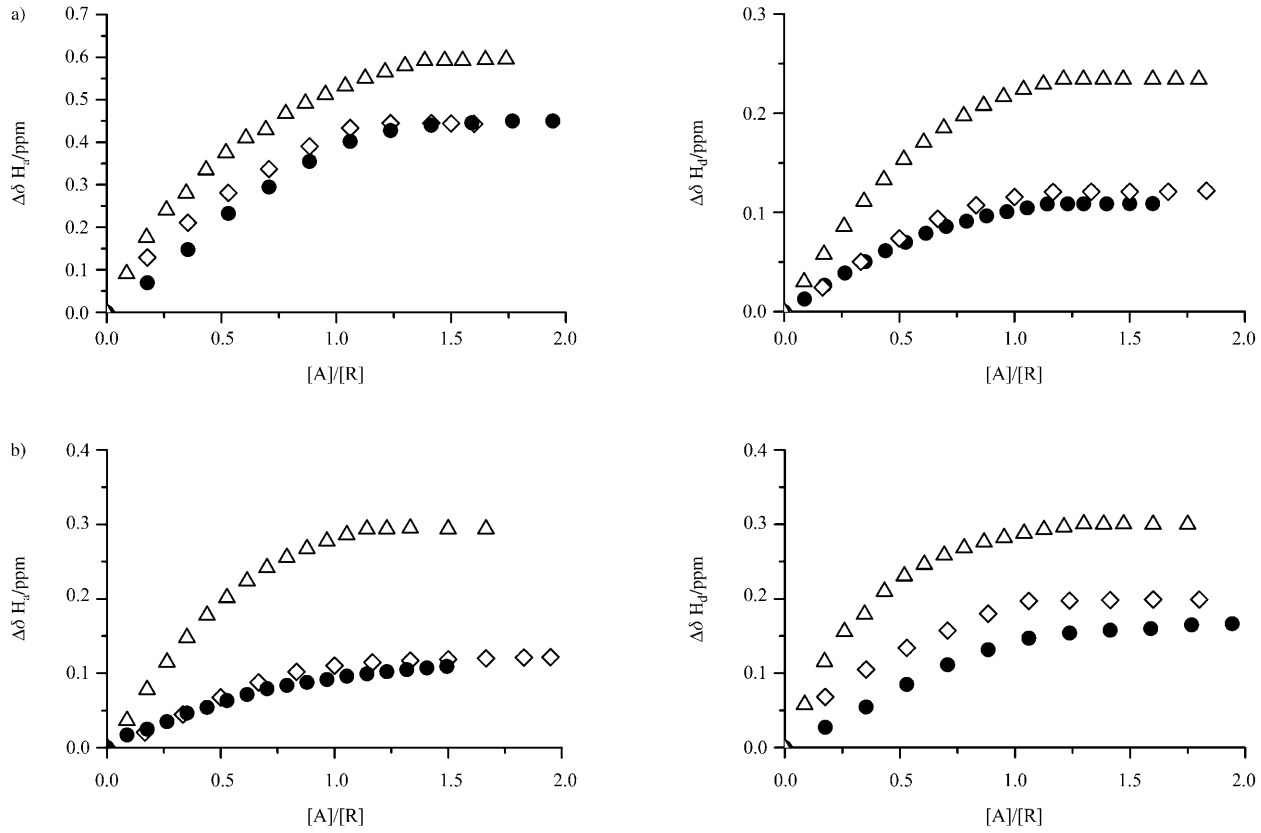

Figure 5. ^{1}H NMR titrations of $\{H_4[32]phen_2N_4\}^{4+}$, $\{H_4[30]phen_2N_6\}^{4+}$ and $\{H_6Me_2[34]phen_2N_6\}^{6+}$ with a) btc^{3-} and b) $ATCP^-$ anions in D_2O; $\Delta\delta$ for H_a (left) and H_d (right) as a function of the number of equivalents of substrate added. The symbols are: $\{H_4[30]phen_2N_6\}^{4+}$ (△), $\{H_6Me_2[34]phen_2N_6\}^{6+}$ (◇) and $\{H_4[32]phen_2N_4\}^{4+}$ (●). The figure is presented in colour in the Supporting Information.

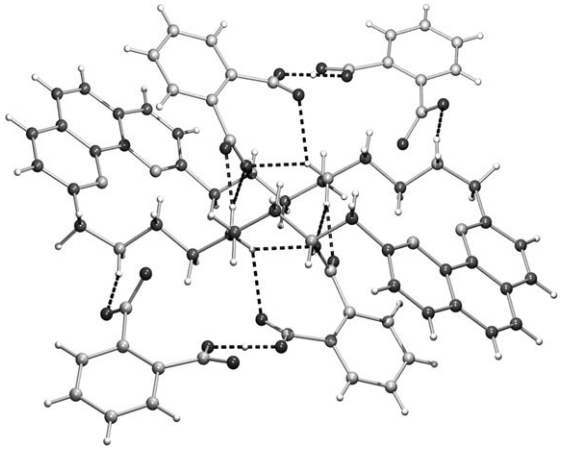

Figure 6. PLUTON view of $[\{H_6[30]phen_2N_6\}][ph(\mu\text{-}H)ph]_2$ showing its overall structure. The figure is presented in colour in the Supporting Information.

The $\{H_6[30]phen_2N_6\}^{6+}$ receptor and the two $[ph(\mu\text{-}H)ph]^{3-}$ dimers are held together in a centrosymmetric binding arrangement by multiple and cooperative N–H···O hydrogen bonds with H···O distances ranging from 1.85 to 2.55 Å. Furthermore, the two $[ph(\mu\text{-}H)ph]^{3-}$ dimer units are clearly located outside of the macrocyclic cavity with the aromatic ring of one of the ph^{2-} units of these two supramolecular entities and the phen rings of the receptor adopting roughly parallel dispositions at interplanar distances of 3.48 Å (see below), which seems to suggest that π–π stacking interactions may also contribute to the stabilisation of the supramolecular association described. The bond lengths and angles found for the receptor are within the range of expected values and the endocyclic torsion angles are consistent with a conformation of ladder-type shape. For both ph^{2-} anions, each carboxylate group displays two non-equivalent C–O distances that vary between 1.230(2) and 1.288(2) Å for the first anion and 1.230(2) and 1.265(2) Å for the second one. In agreement with the formation of a $[ph(\mu\text{-}H)ph]^{3-}$ dimer through a C=O···H···O=C bridge, the longer C–O distances involve two hydrogen-bonded oxygen atoms.

Two different views of the crystal packing diagram of $[\{H_6[30]phen_2N_6\}][ph(\mu\text{-}H)ph]_2{\cdot}8H_2O$ are presented in Figure 7. The first one (top) illustrates the π–π stacking interactions between the phen regions of the receptor and one aromatic ring of the $[ph(\mu\text{-}H)ph]^{3-}$ dimer units established along the [100] crystallographic direction. The corresponding interplanar distances between the centroid of the ph ring and the two phen mean planes are 3.48 and 3.73 Å. The crystal structure can be described as intercalated layers of $\{H_6[30]phen_2N_6\}^{6+}$ and $[ph(\mu\text{-}H)ph]^{3-}$ connected by water molecules through extensive N–H···O and O–H···O hydrogen-bonding interactions (see Figure 7, bottom view) leading to the formation of open channels that accommodate several solvent water molecules.

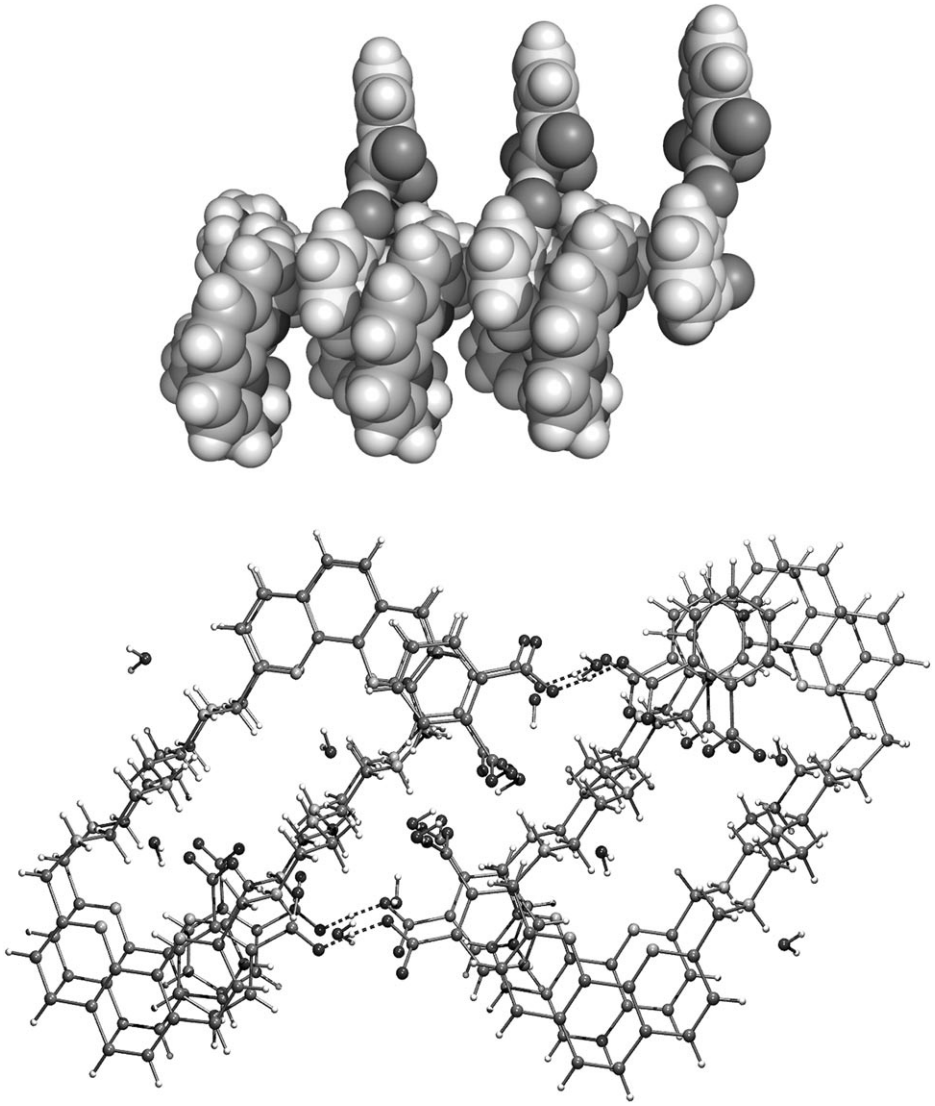

Figure 7. Crystal-packing diagram of $[\{H_6[30]phen_2N_6\}][ph(\mu\text{-}H)ph]_2{\cdot}8H_2O$ showing the $[ph(\mu\text{-}H)ph]^{3-}$ units intercalated between $\{H_6[30]phen_2N_6\}^{6+}$ molecules (top) and the formation of the open channels along the [100] crystallographic direction (bottom). The figure is presented in colour in the Supporting Information.

Molecular modelling studies: Further insights into the binding molecular recognition between the bis-phen macrocyclic receptors $\{H_6Me_2[34]phen_2N_6\}^{6+}$ and $\{H_4[30]phen_2N_6\}^{4+}$ and the anions pyrc$^-$, anthc$^-$, naphc$^-$, btc^{3-} and iph^{2-} were obtained by molecular dynamics (MD) simulations with the GAFF force field[31] within the AMBER 9 software[32] using a water solvent explicit model. As reported above, in solution these two receptors and anions form supramolecular entities of different protonated states. However, the molecular modelling studies were carried out with only the hexa- and tetraprotonated forms of the receptors $\{H_6Me_2[34]phen_2N_6\}^{6+}$ and $\{H_4[30]phen_2N_6\}^{4+}$, respectively, and the fully deprotonated forms of the anions, which are the dominant species in the pH range 4.5–5.0. The anions were selected by taking into account the extension of their aromatic systems and the number of carboxylate groups to evaluate the role of the net charge of the anions, as well as the hydrogen bonding and π–π stacking interactions in the dynamics of the molecular association process.

The docking studies between the receptor and the anion in an equimolar ratio were carried out in the gas phase by MD quenching runs (see the Experimental Section). Two distinct binding scenarios were found. The lowest-energy structures for the associated entity with $\{H_6Me_2[34]phen_2N_6\}^{6+}$ display an open conformation with the two phen moieties twisted with respect to each other (arrangement A). The other significant binding arrangement, B, with a higher energy, adopts a folded conformation with the anion inserted into the macrocyclic cavity between the two phen units, establishing π–π stacking interactions with both phen heads. These two binding arrangements are illustrated in Figure 8 for $\{(H_6Me_2[34]phen_2N_6)(pyrc)\}^{5+}$. For the polyaromatic anions, the energy difference between the B and A arrangements ($E_B - E_A$) decreases with increasing extension of the anion aromatic system, being 31.08, 26.20 and 12.43 kcal mol^{-1} for naphc$^-$, anthc$^-$ and pyrc$^-$, respectively. For the btc^{3-} and iph^{2-} anions this energy difference is 16.68 and 8.80 kcal mol^{-1}, respectively. As found in our preceding studies for $\{(H_5[30]phen_2N_4O_2)(X)\}^{4+}$ (X = pyrc$^-$ and naphc$^-$) complexes,[16] the folded binding arrangement becomes progressively more stable with the enlargement of the aromatic ring, which gives a clear indication that the π–π stacking interactions play an important role in the molecular recognition of the aromatic carboxylate anions (represented in Scheme 2) by the synthetic receptors based on two phen moieties (outlined in Scheme 1). In line with this observation, note that for the $\{H_4[30]phen_2N_6\}^{4+}$ supramolecular entities, the arrangement B is systematically favoured with the naphc$^-$, anthc$^-$ and pyrc$^-$ anions by 8.45, 10.08 and 28.31 kcal mol^{-1}, respectively. For anions with a single aromatic ring this arrangement is stabilised relative to the arrangement A by 2.89 kcal mol^{-1} for btc^{3-} and by 28.43 kcal mol^{-1} for iph^{2-}.

Subsequently, the dynamic behaviour of the associations of $\{H_6Me_2[34]phen_2N_6\}^{6+}$ and $\{H_4[30]phen_2N_6\}^{4+}$ with the pyrc$^-$, anthc$^-$, naphc$^-$, btc^{3-} and iph^{2-} anions was investigated in water solution for 8 ns. As a consequence of the docking results, for the larger receptor two independent simulations were performed by using as starting models the binding arrangements A and B, whereas for the 30-membered macrocycle only the arrangement B was considered. The binding geometry B, with the anion encapsulated between the two phen moieties, is favoured for all $\{H_6Me_2[34]phen_2N_6\}^{6+}$ associated entities, reversing the trend observed in the gas phase. The conversion of A into B was evaluated by measuring the distance between the pyrc$^-$ anion and the two phen rings, as shown in Figure 9.

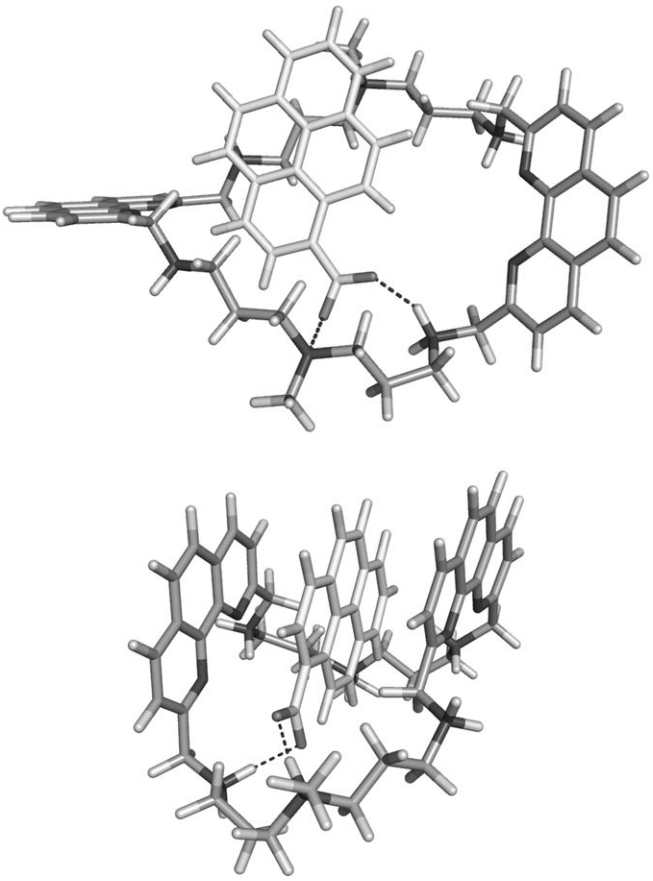

Figure 8. Two alternative binding models found for the docking of $\{(H_6Me_2[34]phen_2N_6)(pyrc)\}^{5+}$: arrangement A (top) and arrangement B (bottom). The figure is presented in colour in the Supporting Information.

It is evident that the open binding conformation (grey line) is retained during the first 0.5 ns of the simulation. After that period, the binding arrangement A is converted into B, which subsequently remains stable until the end of the simulation. On the other hand, the folded binding arrangement B (black line) is stable over the entire course of the simulation. A similar dynamic binding behaviour was observed for $\{(H_6Me_2[34]phen_2N_6)(anthc)\}^{5+}$ and $\{(H_6Me_2[34]phen_2N_6)(btc)\}^{3+}$; the conversion of A into B occurs after 2.5 and 4 ns of simulation, respectively. This suggests that the stability of the open binding arrangement increases with a reduction in the extension of the aromatic system of the substrate, which underlines the role of the aro-

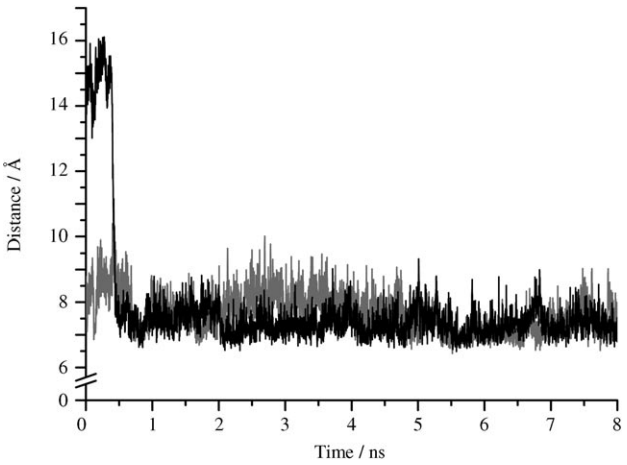

Figure 9. Distances between the centroids defined by the carbon atoms of the phen units for the system $\{(H_6Me_2[34]phen_2N_6)(pyrc)\}^{5+}$ in arrangements A (grey line) and B (black line). The figure is presented in colour in the Supporting Information.

matic system of the anion in the molecular recognition process. Analysis of the hydrogen bonds between $\{H_6Me_2[34]phen_2N_6\}^{6+}$ and $\{H_4[30]phen_2N_6\}^{4+}$ and the five anions (arrangement B) for 8 ns of simulation using a cut-off of 2.5 Å for the H···O distances and 120° for the N–H···O angles showed that the anion-binding is assisted by multiple and cooperative N–H···O hydrogen-bonding interactions. Furthermore, the N–H binding groups of the receptor as well as the oxygen donors of the carboxylate groups involved in the molecular recognition process vary during the molecular dynamics simulation, yielding low occupancies for all potential N–H···O hydrogen-bonding interactions, as exemplified for the association of $\{(H_6Me_2[34]phen_2N_6)(pyrc)\}^{5+}$.[33]. However, in all cases, at least one hydrogen bond is observed throughout the entire simulation period.

Subsequently the binding free energies of the supramolecular associations were estimated in water solution by the MM-PBSA methodology (molecular mechanics/Poisson–Boltzmann surface area).[34] Simulations were also undertaken for the isolated receptors and anions. Thus, three independent trajectories were used in the MM-PBSA calculations to allow the entropic and internal energetic contributions associated with the receptor conformational changes that occur upon binding to be taken into account. The values of the enthalpic and entropic terms of the binding free energies for the geometric arrangement B were calculated with snapshots taken throughout the entire simulation, as described in the Experimental Section, and they are listed in Table 4. The individual contributions to the enthalpic term for each binding association are given in Tables S5 and S6 in the Supporting Information. The enthalpy is basically dictated by the balance between the favourable internal molecular mechanics energy and the unfavourable polar solvation free energy.

As would be expected, the values of the energetic term $T\Delta S$ indicate that the binding of the anions is entropically disfavoured leading to the binding free energies listed in Table 4. The binding free energies calculated for the associations of $pyrc^-$, $anthc^-$, btc^{3-} and iph^{2-} anions with $\{H_4[30]phen_2N_6\}^{4+}$ are overestimated by −3.0, −2.1, −2.3 and −3.4 kcal mol^{-1}, respectively, when compared with those obtained from potentiometric data. The unique exception is the binding association with $naphc^-$ for which the theoretical binding free energy is only 0.1 kcal mol^{-1} higher than the experimental one. The theoretical binding affinity of $\{H_6Me_2[34]phen_2N_6\}^{6+}$ with btc^{3-}, $naphc^-$ and iph^{2-} is underestimated by 2.2, 1.6 and 3.3 kcal mol^{-1}, respectively, whereas the energy difference between the theoretical and experimental binding free energies for $pyrc^-$ and $anthc^-$ is −2.4 and −0.6 kcal mol^{-1}, respectively. Hence, the binding affinity of both receptors for mono-charged aromatics follows the order $pyrc^- > anthc^- > naphc^-$, which indicates that the strength of the binding interaction decreases with a decrease in the extension of the substrate aromatic system. These results show, undoubtedly, the role of π–π stacking interactions in the molecular recognition process of this type of anion. Furthermore, it is also evident that supramolecular association with $\{H_4[30]phen_2N_6\}^{4+}$ is more suitable for accommodating all anions in a folded arrangement.

Finally, when these calculations were repeated for the open binding arrangement A using the portion of the simulation in which this scenario is retained (see above), positive unfavourable values of ΔG_{bind} were obtained. This result leads us to the conclusion that the experimental data corresponds to the folded binding arrangement B, with the encapsulation of the aromatic anions in the macrocyclic cavity.

Conclusion

This work clearly shows that of the three studied receptors, $\{H_j[30]phen_2N_6\}^{j+}$, with a smaller cavity size, is the best for the selective binding of aromatic carboxylate anionic substrates, including the herbicide $ATCP^-$. This receptor is particularly suitable for the uptake of extended aromatic anions, such as $pyrc^-$ and $anthc^-$, or of highly charged anions (btc^{3-}). Indeed, it is capable of sensing and recognising these substrates from a complex mixture of anions that includes other aromatic anions.

Table 4. Energetic contributions to the binding free energies (in kcal mol^{-1}) for the association between the receptors $\{H_6Me_2[34]phen_2N_6\}^{6+}$ and $\{H_4[30]phen_2N_6\}^{4+}$ and five selected anions.

	$\{H_6Me_2[34]phen_2N_6\}^{6+}$						$\{H_4[30]phen_2N_6\}^{4+}$					
Anion	ΔH	σ^*	$T\Delta S$	σ^*	ΔG_{bind}	σ^*	ΔH	σ^*	$T\Delta S$	σ^*	ΔG_{bind}	σ^*
$pyrc^-$	−27.17	0.19	−17.84	0.01	−9.33	0.19	−26.07	0.18	−15.11	0.01	−10.96	0.18
$anthc^-$	−24.50	0.19	−17.44	0.01	−7.06	0.19	−24.91	0.18	−15.25	0.01	−9.66	0.18
$naphc^-$	−18.73	0.19	−17.01	0.02	−1.72	0.19	−18.42	0.17	−13.92	0.01	−4.50	0.17
btc^{3-}	−23.47	0.18	−19.29	0.02	−4.18	0.18	−25.83	0.17	−15.62	0.01	−10.21	0.17
iph^{2-}	−19.15	0.18	−17.69	0.02	−1.46	0.18	−24.19	0.13	−15.32	0.01	−8.87	0.13

[a] σ^* represents the standard deviation from the mean.

This comprehensive study also shows that the dipropylenetriammonium spacers, in spite of their higher positive net charge (+3), are less appropriate than diethylenetriammonium ones (+2) for the design of receptors for the selective binding of aromatic carboxylate anions. Furthermore, experimental binding studies coupled with MD simulations have allowed us to establish that the folded conformation, with the aromatic anion inserted between the phen rings, is the most probable dynamic structure adopted in solution. This arrangement is stabilised by multiple and cooperative interactions, N−H···O hydrogen bonds complemented by π–π stacking interactions.

Experimental Section

General: Microanalyses were carried out by the ITQB Microanalytical Service. The ^{1}H and ^{13}C NMR spectra were recorded with a Bruker CXP 400 spectrometer.

1,10-Phenanthroline-2,9-dicarbaldehyde was prepared by the reaction of 2,9-dimethyl-1,10-phenanthroline with selenium dioxide.[17] 2,2′-Oxydiethylamine was purchased from Acros and hexane-1,6-diamine, diethylenetriamine, *N*,*N*-bis(3-aminopropyl)methylamine and sodium borohydride from Aldrich. All chemicals were of reagent grade and used as supplied. The reference used for the ^{1}H NMR spectra in D_2O was the [D_4]3-(trimethylsilyl)propanoic acid sodium salt. For ^{13}C NMR spectroscopy, dioxane was used as the internal reference.

[32]phen$_2$N$_4$: 1,10-Phenanthroline-2,9-dicarbaldehyde (0.45 g, 1.93 mmol) was dissolved in hot methanol (45 mL) and then cooled to RT. This solution was added dropwise to a methanol solution (25 mL) containing hexane-1,6-diamine (0.28 g, 2.41 mmol) over 10 min. The resulting mixture was stirred overnight. The white solid formed was filtered off and dissolved in ethanol (30 mL). Sodium borohydride (0.3 g, 7.93 mmol) was then added in small portions to the cooled mixture (in an ice bath). Then the solution was stirred for 12 h at RT. The solvent was removed under reduced pressure and the resulting residue was treated with water and repeatedly extracted with chloroform (6×30 mL). The organic phases were combined and completely evaporated under vacuum and then dissolved in ethanol. The pure compound was precipitated from hydrochloric acid solutions as a green powder easy to filter after 12 h at about 4 °C. Yield: 80 %; m.p. 209–210 °C; ^{1}H NMR (400 MHz, D_2O, 25 °C): δ = 1.46 (m, 8H; $NCH_2CH_2CH_2$), 1.81 (m, 8H; $NCH_2CH_2CH_2$), 3.24 (m, 8H; $NCH_2CH_2CH_2$), 4.67 (s, 8H; phenCH_2N), 7.78 (d, 4H; phen), 7.92 (s, 4H; phen), 8.49 ppm (d, 4H; phen); ^{13}C NMR (400 MHz, D_2O, 25 °C, dioxane): δ = 26.9 ($NCH_2CH_2CH_2$), 27.1 ($NCH_2CH_2CH_2$), 49.1 ($NCH_2CH_2CH_2$), 51.5 (phenCH_2N), 124.6, 128.6, 130.4, 140.5, 144.1, 152.8 ppm (phen); MS (ESI): *m*/*z*: 641.4 $[L+H]^+$; elemental analysis calcd (%) for $C_{40}H_{65}C_{l5}N_8O_6$: C 51.59, H 7.04, N 12.23; found: C 51.32, H 7.17, N 12.28.

[30]phen$_2$N$_6$: Diethylenetriamine (0.382 g, 3.70 mmol) was dissolved in methanol (35 mL) and then slowly added dropwise to a cooled methanol (80 mL) solution of 10-phenanthroline-2,9-dicarbaldehyde (0.87 g, 3.68 mmol). The white solid of the macrocyclic Schiff base formed was filtered off and dissolved in ethanol (30 mL). Then the same procedure as described for [32]phen$_2$N$_4$ was used. The rose-coloured pure compound was precipitated as the hydrochloric salt from methanol solution at a low temperature (4 °C). Yield: 60 %; m.p. 229–230 °C; ^{1}H NMR (400 MHz, D_2O, 25 °C): δ = 3.21 (t, 8H; NCH_2CH_2N), 3.48 (t, 8H; NCH_2CH_2N), 4.52 (s, 8H; phenCH_2N), 7.28 (d, 4H; phen), 7.63 (s, 4H; phen), 7.95 ppm (d, 4H; phen); ^{13}C NMR (400 MHz, D_2O, 25 °C, dioxane): δ = 47.9 (NCH_2CH_2N), 48.1 (NCH_2CH_2N), 54.0 (phenCH_2N), 125.1, 129.7, 131.4, 141.6, 145.9, 153.5 ppm (phen); MS (ESI): *m*/*z*: 615.4 $[L+H]^+$; elemental analysis calcd (%) for $C_{36}H_{57}Cl_5N_{10}O_5$: C 48.45, H 6.07, N 15.64; found: C 48.74, H 6.48, N 15.79.

Me$_2$[34]phen$_2$N$_6$: 1,10-Phenanthroline-2,9-dicarbaldehyde (0.65 g, 2.75 mmol) was dissolved in hot methanol (60 mL) and then cooled to RT and then added dropwise into a methanol solution (30 mL) containing *N*,*N*-bis(3-aminopropyl)methylamine (0.40 g, 2.75 mmol) over 10 min. The resulting mixture was stirred for six days and then concentrated to 30 mL under vacuum and sodium borohydride (0.3 g, 8.0 mmol) was added in small portions when the mixture had been cooled in ice bath. After that the solution was stirred for 12 h and then heated at reflux for 5 h. The resulting solution was evaporated, NaOH was added until pH > 8 and then the solution was extracted with chloroform (5×30 mL). The brown oil was dried, precipitated as the hydrochloride salt and recrystallised from hot methanol to give a yellow solid that was dried and stored. Yield: 50 %; m.p. 238–239 °C; ^{1}H NMR (400 MHz, D_2O, 25 °C): δ = 2.36 (m, 8H; $NCH_2CH_2CH_2N$), 2.96 (s, 6H; NCH_3), 3.49 (t, 16H; $NCH_2CH_2CH_2N$), 3.53 (t, 16H; $NCH_2CH_2CH_2N$), 4.71 (s, 8H; phenCH_2N), 7.83 (d, 4H; phen), 8.02 (s, 4H; phen), 8.58 ppm (d, 4H; phen); ^{13}C NMR (400 MHz, D_2O, 25 °C, dioxane): δ = 22.7 ($NCH_2CH_2CH_2N$), 41.5 (NCH_3), 46.3 ($NCH_2CH_2CH_2N$), 53.6 ($NCH_2CH_2CH_2N$), 54.6 (phenCH_2N), 124.6, 128.7, 130.5, 140.6, 145.7, 152.7 ppm (phen); MS (ESI): *m*/*z*: 699.46 $[L+H]^+$; elemental analysis calcd (%) for $C_{42}H_{78}Cl_6N_{10}O_9$: C 46.71, H 7.28, N 12.97; found: C 46.55, H 7.66, N 13.27.

Crystals of [{H$_6$[30]phen$_2$N$_6$}][ph(μ-H)ph]$_2$·8H$_2$O: Potassium hydrogen phthalate (2.5 equiv, 40 mL, 7×10^{-2} M) in D_2O was added to a solution of the receptor $\{H_4[30]phen_2N_6\}^{4+}$ (600 μL, 5.5×10^{-3} M) in D_2O and the pD adjusted to 3.2. The solution was left in the NMR tube at RT and brown crystals were obtained in 3 days.

Preparation of the anionic substrates: A 1.0 M aqueous potassium hydroxide solution (1.0–3.0 equiv depending on the number of acidic functions) was added to a stirred aqueous solution of the acid form of the substrates (10.0 mmol, 20 mL). The solvent was then evaporated and the salts were recrystallised from acetone and dried under vacuum.

Potentiometric measurements

Reagents and solutions: The potentiometric titrations were carried out in H_2O or H_2O/MeOH (50:50, v/v) solutions at 298.2±0.1 K using KCl (0.10 M) as the supporting electrolyte. The solutions of the anions were standardised by titration with a standard HCl solution. Carbonate-free solutions of KOH were freshly prepared in H_2O or H_2O/MeOH (50:50, v/v) by dilution of concentrated solutions of titrisol ampoule (Merck), maintained in a closed bottle and discarded when the percentage of carbonate was about 0.5 % of the total amount of base, as verified by the Gran method.[35] The demineralised water used was obtained from a Millipore/Milli-Q system.

Equipment and working conditions: The equipment used has been described previously.[36] The temperature was kept at 298.2±0.1 K. Atmospheric CO_2 was excluded from the cell during the titration by passing purified nitrogen across the top of the solution in the reaction cell.

Measurements: The $[H^+]$ of the solutions was determined by the measurement of the electromotive force of the cell, $E = E'^{\ominus} + Q\log[H^+] + E_j E'^{\ominus}$. Q, E_j and $K_w = [H^+][OH^-]$ were obtained as described previously.[36] The term pH is defined as $-\log[H^+]$. The value of K_w was found to be equal to $10^{-13.80}$ M^2 in aqueous solution and $10^{-13.91}$ M^2 in H_2O/MeOH (50:50, v/v).[37] The measurements were carried out by using 20.00 mL of $\approx2.0\times10^{-3}$ M receptor solutions and the substrate concentration was varied from 2×10^{-3} to 5×10^{-3} M. At least three titrations were performed in the 2–10 pH range at receptor (R)/anion (A) concentration ratios of 1:1, 1:2 and 1:3.

Calculation of equilibrium constants: The protonation constants of the three macrocycles and of all the substrates, $\beta_{H_hL_l} = [H_hL_l]/[H]^h[L]^L$, were determined from the experimental data by using the HYPERQUAD program.[20] All these constants were taken as fixed values in order to obtain the equilibrium constants of the associated species from the experimental data corresponding to titrations of different R/A ratios. The different titration curves of the same system were first considered as a single set and finally all the data were merged together and simultaneously evaluated to give the final model of binding constants. In addition, back titrations (from alkaline to acid pH) were also performed to check the reversibility of the reactions. The initial computations were obtained in the

form of overall stability constants, $\beta_{H_hL_lA_a}=[H_hL_lA_a]/[H]^h[L]^l[A]^a$. The errors quoted are the standard deviations of the stability constants given directly by the program for the input data, which include all the experimental points of all the titration curves. The species considered in a particular model were those that could be justified by the principles of supramolecular chemistry.

^{1}H NMR spectroscopic titrations

Reagents and solutions: The concentrations of [32]$phen_2N_4$, [30]$phen_2N_6$ and Me_2[34]$phen_2N_6$ (0.01 M) solutions in D_2O were determined by titration with DCl (0.1 M in D_2O) or CO_2-free KOD freshly prepared (0.10 M). Solutions of $\{H_4[32]phen_2N_4\}^{4+}$, $\{H_4[30]phen_2N_6\}^{4+}$ and $\{H_6Me_2[34]phen_2N_6\}^{6+}$ (2.0×10^{-3} M) were prepared by dissolution of the macrocycles in 0.5 mL of D_2O and then the pD was adjusted to $\approx$5.0. The anion solutions were prepared at $1.2–2.2\times10^{-2}$ M by dissolution of the potassium salts in 0.5 mL of D_2O. The potassium salt of each anion dissolved D_2O was added in portions of 0.01 mL to solutions of the prepared receptors in D_2O at 298.2 K by using a Hamilton syringe (Microliter 700 series of 25 μL). About 15 additions were necessary for each titration until no further change in the chemical shift was observed, and each solution was left 15–20 min to stabilise. No effort was made to maintain a constant ionic strength, but care was taken to maintain the pD value within a range of $\pm$0.25 and to avoid CO_2 absorption from the atmosphere. The pH* = $-\log$[H*] (pH* refers to the value directly measured in the pH meter of solutions in D_2O upon calibration with buffers prepared in H_2O) values were directly measured in the NMR tube with a microelectrode Hamilton SpinTrode coupled with an Orion 420A instrument. The pH meter was calibrated with aqueous buffered solutions at pH 7.20 and 4.00. The final pD was calculated from pD = pH* + (0.40 ± 0.02).[22b] The NOESY experiments were performed by collecting $1024(t_2)\times512(t_1)$ data points by using standard Bruker pulse programs. A 5.0 μs pulse width corresponding to a 90° flip angle and a mixing time of 150 ms was used for the receptor (pD = 4.95) and 500 ms for the supramolecular entities.

Determination of the association constants: Changes in the chemical shifts of all the protons were recorded and the association constants of the various species formed in solution were determined from the experimental data by using HypNMR,[21] which requires as input the concentration of each component and the observed chemical shift. Initial calculations provided the overall stability constants $\beta_{R_rA_a}$ ($\beta_{R_rA_a}=[R_rA_a]/[R]^r[A]^a$, with R = $\{H_4[32]phen_2N_4\}^{4+}$, $\{H_4[30]phen_2N_6\}^{4+}$ and $\{H_6Me_2[34]phen_2N_6\}^{6+}$). Only species with a 1:1 stoichiometry were found in all cases. The errors quoted are the standard deviations of the overall stability constants given directly by the program from the input data, which includes the experimental points for most of the resonances of each compound.

Job plots: Stock solutions of the receptors (conc. from 2.00 to 3.00 mM) and the potassium salts of the substrates (under the same concentrations) were prepared in D_2O. Ten NMR tubes were filled with 500 μL solutions of the receptor and substrate in the following volume ratios: 50:450, 100:400, 150:350, 200:300, 250:250, 300:200, 350:150, 400:100, 450:50 and 500:0. The changes in the chemical shifts of the resonances for each solution were measured and then the plot of the product between the increment in the chemical shift and the receptor concentration as a function of the molar fraction of the receptor was performed. The maximum of the curve indicates the stoichiometry of the new entity formed. $[C]=[R]_0(\delta_{obs}-\delta_R)/(\delta_{max}-\delta_R)$, in which $[R]_0$ is the total receptor concentration, δ_{obs} is the observed chemical shift, δ_R is the chemical shift of the free receptor and δ_{max} is the chemical shift of the associated entity. As $(\delta_{max}-\delta_R)$ is a constant, the concentration of the associated entity is proportional to $\Delta\delta[R]_0$ [with $\Delta\delta=(\delta_{obs}-\delta_R)$]. All these curves exhibit one maximum at $X=0.5$, which indicates a 1:1 stoichiometry for the associated species.[26] The plots of [30]$phen_2N_6$ as a function of ph^{2-}, and of Me_2[34]$phen_2N_6$ as a function of btc^{3-} are presented in Figure S3 in the Supporting Information, as typical examples.

Crystallography: The X-ray data for $[\{H_6[30]phen_2N_6\}][ph(\mu\text{-}H)ph]_2\cdot8H_2O$ were collected on a CCD Bruker APEX II instrument at 100(2) K using graphite monochromatised $Mo_{K\alpha}$ radiation ($\lambda=0.71073$ Å). The crystal was positioned at 35 mm from the CCD and the spots were measured by using a counting time of 80 s. Data reduction and empirical absorption were carried out by using the SAINT-NT software package from Bruker AXS. The structure was solved by direct methods and subsequent difference Fourier syntheses and refined by full-matrix least-squares on F^2 by using the SHELX-97 suite of programs.[38] Anisotropic thermal parameters were used for all non-hydrogen atoms. Hydrogen atoms bonded to carbon and nitrogen atoms were placed at calculated positions. The atomic positions of the hydrogen atoms of the water molecules and the O–(μ-H)–O bridging hydrogen atoms were taken from difference Fourier maps. The water hydrogen atoms were refined with O–H distances restrained to 0.83 Å. All hydrogen atoms were refined with $U_{iso}=1.2U_{eq}$ of the parent atom except for the bridging hydrogen, which was refined with isotropic thermal parameters. The residual electronic density ranging from -0.404 to 0.530 e Å^{-3} was within the expected values. Molecular diagrams were drawn with PLATON.[39] The crystal data are summarised in Table S7 in the Supporting Information. CCDC-688493 contains the supplementary crystallographic data for this paper. These data can be obtained free of charge from The Cambridge Crystallographic Data Centre via www.ccdc.cam.ac.uk/data_request/cif

Molecular dynamics simulations: Molecular modelling simulations and free-energy calculations were performed with AMBER 9[32] with the atomic parameters taken from the GAFF force field.[31] The starting models for $\{H_6Me_2[34]phen_2N_6\}^{6+}$ and $\{H_4[30]phen_2N_6\}^{4+}$ were generated from the crystal structure of [30]$phen_2N_4O_2$.[16] The partial atomic charges for the receptors and anions ($pyrc^-$, $naphc^-$, btc^{3-}, iph^{2-} and $anthc^-$) were calculated by using the Gaussian 03 program[40] at the HF/6-31G(d) level of theory with the RESP methodology.[41] Docking between the receptor and the anion, with a stoichiometry of 1:1, was investigated by using molecular dynamics quenching runs as follows: the initial structures were energy-minimised by molecular mechanics calculations and subsequently submitted to a MD run at 2000 K in the gas phase for 1 ns using a time step of 1 fs. A total of 10000 conformations were generated and then minimised by MM.

For each supramolecular system two different binding arrangements were selected and solvated using the TIP3P water model, giving cubic boxes containing between 2231 and 2832 water molecules. The isolated anions and receptors were also solvated to give three independent simulations for free-energy calculations. The electrostatic neutrality of the systems was achieved by the replacement of water molecules by the equivalent number of chloride anions depending on the total charge of the system. The chloride anions were described with force-field parameters taken from ref. [42]. The systems were equilibrated with a multistage protocol composed of two successive MM energy minimisations to eliminate undesired contacts. An NVT (constant number of particles, volume and temperature) simulation for 50 ps was run to increase the temperature from 0 to 300 K and, finally, an NPT (constant number of particles, pressure and temperature) simulation over 150 ps to adjust the system's density to the experimental density of liquid water at the considered temperature. After the equilibration process, the dimensions of the boxes were in the range of 40.9–48.3 Å. Finally, the MD data collection was run for 8 ns using an NPT ensemble and a time step of 2 fs. The bonds involving hydrogen atoms were constrained by using the SHAKE algorithm, the long-range electrostatic interactions were described by the Particle Mesh Edwald method and the non-bonding van der Waals interactions were subjected to a 12 Å cut-off. Frames were saved every 0.2 ps throughout the MD simulation.

The binding free energy between the two receptors and the five aromatic anions were calculated by post-processing the trajectory files of the individual simulations carried out with assembled species and the isolated receptors and anions by using the MM-PBSA (Molecular Mechanics/Poisson–Boltzmann Surface Area) methodology.[34] The enthalpic contributions were determined by solving the Poisson–Boltzmann equations by the Delphi approach[43] with a solute interior dielectric constant set to 2.0 and 3.0, which are acceptable values for small organic molecules. However, generally, the free binding energies calculated with the smaller value display a better fitting with the experimental ones. The entropic contributions were determined through normal mode analysis, as implemented in AMBER 9.[32] The average binding free energy was calculated by using

4000 binding scenarios extracted with a frequency of 10 from the MD trajectories. Molecular diagrams were drawn with PyMOL.[44]

Acknowledgements

The authors acknowledge the Fundação para Ciência e Tecnologia (FCT) with co-participation of European Community funds FEDER for financial support under projects PTDC/QUI/56569/2004 and PTDC/QUI/68582/2006. C.C. and V.C. thank the FCT for Ph. D. grants (SFRH/BD/19266/2004 and SFRH/BD/38075/2007, respectively).

[1] J. W. Steed, D. R. Turner, K. Wallace, *Core Concepts in Supramolecular Chemistry and Nanochemistry*, Wiley, New York, **2007**.
[2] E. García-España, P. Díaz, J. M. Llinares, M. P. Clares, A. Bianchi, *Coord. Chem. Rev.* **2006**, *250*, 2952–2986.
[3] A. Bianchi, K. Bowman-James, E. García-España, *Supramolecular Chemistry of Anions*, Wiley, New York, **1997**.
[4] R. Celis, M. C. Hermosi, L. Cornejo, M. J. Carrizosa, J. Cornejo, *Int. J. Environ. Anal. Chem.* **2002**, *82*, 503–517.
[5] G. Welp, G. W. Brukmmer, *Ecotoxicol. Environ. Saf.* **1999**, *43*, 83–90.
[6] C. M. Gonçalves, J. C. G. E. Silva, M. F. Alpendurada, *J. Agric. Food Chem.* **2007**, *55*, 6227–6235.
[7] H. Schneider, A. K. Yatsimirsky, *Chem. Soc. Rev.* **2008**, *37*, 263–277.
[8] P. A. Gale, S. E. Garcia-Garrido, J. Garric, *Chem. Soc. Rev.* **2008**, *37*, 151–190.
[9] G. V. Oshovsky, D. N. Reinhoudt, V. Willem, *Angew. Chem.* **2007**, *119*, 2418–2445; *Angew. Chem. Int. Ed.* **2007**, *46*, 2366–2393.
[10] C. A. Ilioudis, J. W. Steed, *J. Supramol. Chem.* **2001**, *1*, 165–187.
[11] C. Anda, M. A. Martínez, A. Llobet, *Supramol. Chem.* **2005**, *17*, 257–266.
[12] K. Wichmann, B. Antonioli, T. Söhnel, M. Wenzel, K. Gloe, K. Gloe, J. R. Price, L. F. Lindoy, A. J. Blake, M. Schröder, *Coord. Chem. Rev.* **2006**, *250*, 2987–3003.
[13] K. Bowman-James, *Acc. Chem. Res.* **2005**, *38*, 671–678.
[14] P. A. Gale, R. Quesada, *Coord. Chem. Rev.* **2006**, *250*, 3219–3244.
[15] W. J. Belcher, M. Fabre, T. Farhan, J. W. Steed, *Org. Biomol. Chem.* **2006**, *4*, 781–786.
[16] C. Cruz, R. Delgado, M. G. B. Drew, V. Félix, *J. Org. Chem.* **2007**, *72*, 4023–4034.
[17] C. Chandler, J. L. W. Deady, J. A. Reiss, *J. Heterocycl. Chem.* **1981**, *18*, 599–601.
[18] K. E. Krakowiak, J. S. Bradshaw, W. Jiang, N. K. Dalley, G. Wu, R. M. Izatt, *J. Org. Chem.* **1991**, *56*, 2675–2680.
[19] J. S. J. Keipert, C. B. Knobler, D. J. Cram, *Tetrahedron* **1987**, *43*, 4861–4874.
[20] P. Gans, A. Sabatini, A. Vacca, *Talanta* **1996**, *43*, 1739–1753.
[21] C. Frassineti, S. Ghelli, P. Gans, A. Sabatini, M. S. Moruzzi, A. Vacca, *Anal. Biochem.* **1995**, *231*, 374–382.
[22] a) R. Delgado, J. J. R. Fraústo da Silva, M. T. S. Amorim, M. F. Cabral, S. Chaves, J. Costa, *Anal. Chim. Acta* **1991**, *245*, 271–282; b) H. Galster, *pH Measurement, Fundamentals, Methods, Applications, Instrumentation*, VCH, Weinheim, **1991**.
[23] L. Alderighi, P. Gans, A. Ienco, D. Peters, A. Sabatini, A. Vacca, *Coord. Chem. Rev.* **1999**, *184*, 311–318.
[24] J. Pina, J. Seixas de Melo, F. Pina, C. Lodeiro, J. C. Lima, A. J. Parola, C. Soriano, M. P. Clares, M. T. Albelda; M. A. B. E. García-España, M. L. Godino-Salido, V. L. Santiago, M. J. Melo, F. Pina, C. Soriano, *J. Chem. Soc. Perkin Trans. 2* **1999**, 2545–2549, R. Aucejo, E. García-España, *Inorg. Chem.* **2005**, *44*, 7449–7458.
[25] L. D. Pettit, H. K. J. Powell, *IUPAC Stability Constants Database*, Academic Software, Timble, version 5, **2003**.
[26] a) L. Sebo, F. Diederich, V. Gramlich, *Helv. Chim. Acta* **2000**, *83*, 93–113; b) K. Hirose, *J. Inclusion Phenom. Macrocyclic Chem.* **2001**, *39*, 193–209.
[27] M. T. Albelda; M. A. B. E. García-España, M. L. Godino-Salido, V. L. Santiago, M. J. Melo, F. Pina, C. Soriano, *J. Chem. Soc. Perkin Trans. 2* **1999**, 2545–2549.
[28] J. A. Aguilar, B. Celda, V. Fusi, E. García-España, V. L. Santiago, M. C. Martínez, J. A. Ramírez, C. Soriano, R. Tejero, *J. Chem. Soc. Perkin Trans. 2* **2000**, 1323–1328.
[29] A. Bianchi, E. Garcia-España, *J. Chem. Educ.* **1999**, *76*, 1727–1732.
[30] F. H. Allen, *Acta Crystallogr. Sect. B* **2002**, *58*, 380–388.
[31] J. Wang, R. M. Wolf, J. W. Caldwell, P. A. Kollman, D. A. Case, *J. Comput. Chem.* **2004**, *25*, 1157–1174.
[32] D. A. Case, T. A. Darden, T. E. Cheatham III, C. L. Simmerling, J. Wang, R. E. Duke, R. Luo, K. M. Merz, D. A. Pearlman, M. Crowley, R. C. Walker, W. Zhang, B. Wang, S. Hayik, A. Roitberg, G. Seabra, K. F. Wong, F. Paesani, X. Wu, S. Brozell, V. Tsui, H. Gohlke, L. Yang, C. Tan, J. Mongan, V. Hornak, G. Cui, P. Beroza, D. H. Mathews, C. Schafmeister, W. S. Ross, P. A. Kollman, AMBER 9, University of California, San Francisco (USA), **2006**.
[33] For the binding association in $\{(H_6Me_2[34]phen_2N_6)(pyrc)\}^{5+}$, four hydrogen bonds between the anion carboxylate group and several N–H groups of the macrocyclic receptor were established during the simulation (8 ns). Two of the hydrogen bonds had average H···O distances of 1.94 and 1.92 Å, average N–H···O angles of 159 and 162° and occupancies of 48 and 26%, respectively. The remaining two hydrogen bonds were considerably weaker with average H···O distances of 2.49 and 2.30 Å, average N–H···O angles of 124 and 158° and occupancies of 31 and 21%, respectively.
[34] P. A. Kollman, I. Massova, B. Kuhn, S. Huo, L. Chong, M. Lee, T. Lee, Y. Duan, W. Wang, O. Donni, P. Cieplak, J. Srinivasan, D. A. Case, T. E. Cheatham III, *Acc. Chem. Res.* **2000**, *33*, 889–897.
[35] a) G. Gran, *Analyst* **1952**, *77*, 661–671; b) F. J. Rossotti, H. J. Rossotti, *J. Chem. Educ.* **1965**, *42*, 375–378.
[36] S. Carvalho, R. Delgado, M. G. B. Drew, V. Calisto, V. Félix, *Tetrahedron* **2008**, *64*, 5392–5403.
[37] F. Li, R. Delgado, M. G. B. Drew, V. Félix, *Dalton Trans.* **2006**, 5396–5403.
[38] G. M. Sheldrick, SHELX-97, University of Göttingen, Göttingen, **1997**.
[39] L. Spek, PLATON, *A Multipurpose Crystallographic Tool*, Utrecht University, Utrecht (Netherlands), **2003**.
[40] Gaussian 03, Revision B.04, M. J. Frisch, G. W. Trucks, H. B. Schlegel, G. E. Scuseria, M. A. Robb, J. R. Cheeseman, J. A. Montgomery, Jr., T. Vreven, K. N. Kudin, J. C. Burant, J. M. Millam, S. S. Iyengar, J. Tomasi, V. Barone, B. Mennucci, M. Cossi, G. Scalmani, N. Rega, G. A. Petersson, H. Nakatsuji, M. Hada, M. Ehara, K. Toyota, R. Fukuda, J. Hasegawa, M. Ishida, T. Nakajima, Y. Honda, O. Kitao, H. Nakai, M. Klene, X. Li, J. E. Knox, H. P. Hratchian, J. B. Cross, V. Bakken, C. Adamo, J. Jaramillo, R. Gomperts, R. E. Stratmann, O. Yazyev, A. J. Austin, R. Cammi, C. Pomelli, J. W. Ochterski, P. Y. Ayala, K. Morokuma, G. A. Voth, P. Salvador, J. J. Dannenberg, V. G. Zakrzewski, S. Dapprich, A. D. Daniels, M. C. Strain, O. Farkas, D. K. Malick, A. D. Rabuck, K. Raghavachari, J. B. Foresman, J. V. Ortiz, Q. Cui, A. G. Baboul, S. Clifford, J. Cioslowski, B. B. Stefanov, G. Liu, A. Liashenko, P. Piskorz, I. Komaromi, R. L. Martin, D. J. Fox, T. Keith, M. A. Al-Laham, C. Y. Peng, A. Nanayakkara, M. Challacombe, P. M. W. Gill, B. Johnson, W. Chen, M. W. Wong, C. Gonzalez, J. A. Pople, Gaussian, Inc., Wallingford CT, **2004**.
[41] C. I. Bayly, P. Cieplak, W. D. Cornell, P. A. Kollman, *J. Phys. Chem.* **1993**, *97*, 10269–10280.
[42] J. R. Blas, M. Márquez, J. L. Sessler, F. Javier Luque, M. Orozco, *J. Am. Chem. Soc.* **2002**, *124*, 12796–12805.
[43] W. Rocchia, E. Alexov, B. Honig, *J. Phys. Chem. B* **2001**, *105*, 6507–6514.
[44] W. L. DeLano, The PyMOL Molecular Graphics System DeLano Scientific, San Carlos, **2002**, http://www.pymol.org

Received: May 23, 2008
Revised: November 7, 2008
Published online: February 5, 2009

